Allosteric role of the large-scale domain opening in biological catch-binding

Yuriy V. Pereverzev,* Oleg V. Prezhdo,†,* and Evgeni V. Sokurenko‡
Departments of Chemistry and Microbiology, University of Washington, Seattle, Washington 98195, USA
(Received 9 December 2008; published 18 May 2009)

The proposed model demonstrates the allosteric role of the two-domain region of the receptor protein in the increased lifetimes of biological receptor/ligand bonds subjected to an external force. The interaction between the domains is represented by a bounded potential, containing two minima corresponding to the attached and separated conformations of the two protein domains. The dissociative potential with a single minimum describing receptor/ligand binding fluctuates between deep and shallow states, depending on whether the domains are attached or separated. A number of valuable analytic expressions are derived and are used to interpret experimental data for two catch bonds. The P-selectin/P-selectin-glycoprotein-ligand-1 (PSGL-1) bond is controlled by the interface between the epidermal growth factor (EGF) and lectin domains of P-selectin, and the type 1 fimbrial adhesive protein (FimH)/mannose bond is governed by the interface between the lectin and pilin domains of FimH. Catch-binding occurs in these systems when the external force stretches the receptor proteins and increases the interdomain distance. The allosteric effect is supported by independent measurements, in which the domains are kept separated by attachment of another ligand. The proposed model accurately describes the experimentally observed anomalous behavior of the lifetimes of the P-selectin/PSGL-1 and FimH/mannose complexes as a function of applied force and provides valuable insights into the mechanism of catch-binding.

DOI: 10.1103/PhysRevE.79.051913 PACS number(s): 87.15.La, 05.70.Ln, 87.64.Dz

I. INTRODUCTION

The allosteric control over receptor/ligand binding came under active scrutiny following the works of Monod *et al.* [1] and Koshland *et al.* [2] (see recent review [3]). These papers showed that a control molecule, activator or inhibitor, bound far away from the active site changed the site's affinity toward a ligand of interest. The microscopic picture [4–6] of this phenomenon is rationalized by the fact that binding at the allosteric site produces stresses that are propagated through globular protein structure and cause static or dynamics changes in the distant active site. Recently, another form of allosteric control over enzyme's activity has been explored. Instead of the molecular activator or inhibitor, the allosteric subsystem can be controlled by force. For instance, a mechanical stress on the allosteric subunit can be exerted by short pieces of DNA of varying length [7–10].

The force-controlled allosteric effect on receptor/ligand binding is quite hard to detect. The force typically acts on the allosteric subunit through the bond itself because receptor/ligand systems are usually stretched by pulling at the receptor and ligand ends. If experiments reveal a regular slip bond, i.e., the bond lifetime decreases with applied force, both the force and a possible allosteric effect operate in unison, making the bond less stable. As a result, the overall response of the bond to the force is well described by a single Bell-type expression [11], representing lowering of the bond-dissociation barrier by force, regardless of the allosteric mechanism. So-called catch bonds become more stable with applied force [12,13], up to a certain force value. They present a much better chance for detecting the force-induced allostery. In this case, the allosteric mechanism acts to increase the bond lifetime, while the force facilitates bond rupture.

The original theoretical proposal of Dembo *et al.* [14] that a biological receptor/ligand bond can become more stable, when stretched by an outside force, has found experimental confirmation only in recent years. This unusual form of binding, catch-binding, was discovered in the type 1 fimbrial adhesive protein (FimH)/mannose [15], P- and L-selectins/P-selectin-glycoprotein-ligand-1 (PSGL-1) [12,16], and actin/myosin [17] complexes. In all three cases, the bond lifetime first increases with force strength, showing catch-binding, but then reaches a maximum and drops as in ordinary slip bonds.

Several proposed models suggest alternative interpretations for this anomalous phenomenon and provide equally accurate quantitative description of the experimental data [18–25]. The majority of the models assume that the catch and slip regimes correspond to two distinct dissociation pathways. In the slip pathway, the ligand moves along the direction of the applied force and, therefore, the slip barrier lowers as the force increases. During dissociation along the catch pathway, the ligand moves against the direction of the force and, hence, the catch barrier grows with increasing force. In order to observe catch-binding within over a broad range of force strengths, the two-pathway potential should satisfy the following two conditions. First, the catch barrier must be lower than the slip barrier in the absence of the force. This guarantees that, initially, at zero force, the ligand is more likely to escape the binding site via the catch pathway. As the force increases, the catch barrier grows and the slip barrier drops. To stabilize the bond, the growth of the catch barrier should outpace the decrease in the slip barrier. According to the Bell mechanism [11], the changes in the barrier heights are proportional to the barrier widths. Therefore, in order to

*Department of Chemistry
†Corresponding author; prezhdo@u.washington.edu
‡Department of Microbiology

observe catch-binding, the catch barrier must be wider than the slip barrier. This is the second condition. At some force, the heights of the two barriers become equal. With further force increases, the slip barrier drops below the catch barrier, and the bond behaves as an ordinary slip bond.

The simplest version of the two-pathway model of the biological catch bond is presented in Ref. [21]. The model uses only one bound state and contains only four parameters. A number of analytic results and universal relationships can be obtained for the simplest two-pathway model [26–28], assisting in the analysis and interpretation of the experimental data. In order to rationalize additional experimental details, more complex versions of the two-pathway model containing two bound states have been developed [19,20,22]. In all cases catch-binding is obtained in the regime satisfying the two conditions described above. The catch barrier should be initially lower and should rise faster than the slip barrier.

An alternative interpretation of catch-binding is presented in Ref. [25]. Rather than postulating two different dissociation pathways, this model explains the phenomenon by a force-induced deformation of the binding pocket. In catch bonds the deformation favors binding by adjusting protein conformations, improving the receptor/ligand fit and increasing the interaction. In slip bonds the deformation disfavors binding by worsening the fit and decreasing the interaction. Stated in terms of an interaction potential, the deformation model implies that both the top of the dissociation barrier and the bottom of the bound-state minimum are lowered by the applied force. It is essential for catch-binding that within a certain force range the minimum is lowered faster than the maximum. The bottom of the bound-state minimum and the top of the dissociation barrier are brought down by different physical mechanisms, by the bond deformation and the Bell mechanism, respectively. In contrast, the two-pathway model employs only the Bell mechanism and does not consider force-induced changes in the receptor/ligand interaction. The deformation model [25] reproduces the catch phenomenon using just one bond-dissociation pathway and can be viewed as a specific realization of the induced receptor/ligand fitting idea [29]. Compared to the two-pathway model, which achieves catch-binding with rigid receptor and ligand, the deformation model explains the effect by protein elasticity.

References [13,15,30–32] investigated the complex between the FimH protein and mannose, and showed it to be a catch bond. The bond lifetime first increased and then decreased with growing force. The authors established the allosteric role of the lectin/pilin subunit in increasing the receptor/ligand binding affinity. They found that the FimH/mannose bond was weak when the two domains were attached. On the contrary, when the domains were kept separated by another molecule that inserted between the domains, the bond strengthened [31]. Computer simulations [33,34] indicated a similar force-induced stretching of the interface between the epidermal growth factor (EGF) and lectin domains in the P-selectin/PSGL-1 complex, suggesting that the allosteric effect could be important in this system as well. The most recent experimental work [35,36] that appeared after this paper was submitted for publication provided further support for the allosteric basis of catch-binding in the selectin systems.

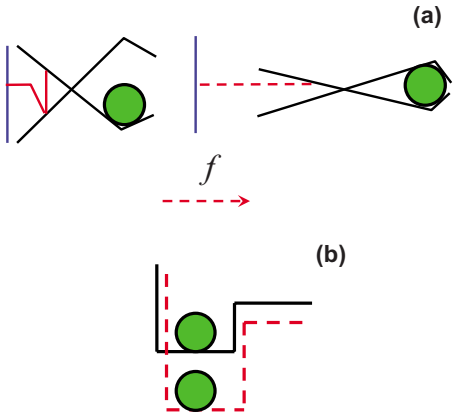

FIG. 1. (Color online) Schematic of the allosteric deformation model. (a) The receptor, solid and dashed lines, is pulled at one end and undergoes a large-scale conformational change. The interdomain fragment is originally closed (solid red lines) and stretched with applied force (dash red line). Simultaneously, the binding pocket at the other end of the receptor closes, creating a tighter fit for the ligand (green circle). (b) The change in the binding pocket induced by the stretching of the interdomain fragment deepens the receptor/ligand interaction potential (dashes).

The current work presents a mathematical formulation of the allosteric catch-binding and illustrates this effect with the FimH/mannose and P-selectin/PSGL-1 bonds. Conceptually, the allosteric model is close to the deformation model [25]. The stretching of the interdomain interface, together with the associated changes the shape of the binding pocket, can be regarded as a particular bond deformation. The allosteric deformation of the catch bond starts as a large-scale conformational rearrangement of the receptor protein. Then, the created change in the orientation of the two domains propagates to the binding pocket and improves the receptor/ligand interaction.

II. THEORY

The key constituents of the allosteric catch-binding model are presented schematically in Fig. 1. Part (a) depicts the receptor/ligand pair, represented by the lines and the green circle, respectively. The black lines depict the lectin domain. The blue line shows the pilin domain in FimH or the EGF domain in P-selectin. The red line represents the fragment connecting the two domains. Initially, left panel, the domains are attached, and the binding pocket containing the ligand is open. The force acting on the receptor and ligand termini stretches the fragment connecting the two domains, and the solid red line transforms into the dashed red line in Fig. 1(a). As a result, the two domains separate. This large-scale conformational change propagates to the binding pocket and makes it tighter, better matching the size of the ligand. Part (b) of Fig. 1 shows the receptor/ligand binding potential. The allosteric deformation of the binding pocket lowers the bound-state minimum. Figure 1 is a simple diagram, meant to illustrate the basic concept underlying the allosteric model of the biological catch bond. The details of the model are worked out below, first, for the two-domain subunit, and then, for the receptor/ligand interaction.

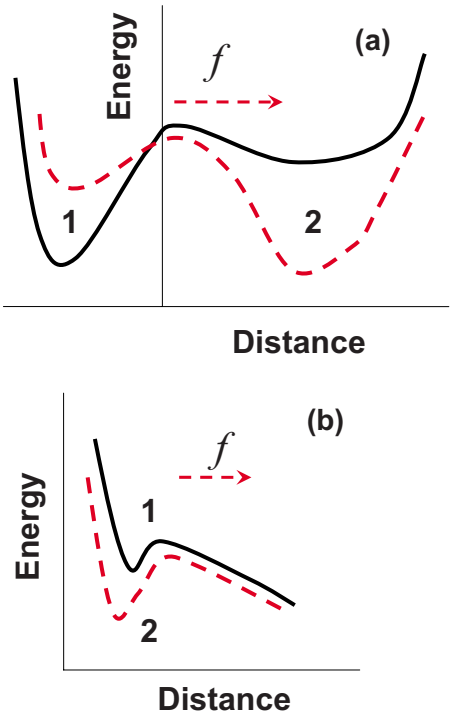

FIG. 2. (Color online) Potential energy profiles describing (a) opening of the interdomain fragment and (b) receptor/ligand interaction. The solid and dashed lines show potentials for the limiting cases of attached and separated domains, $f=0$ and $f\neq 0$, states "1" and "2," respectively. Subjected to the force (dashed arrow), the system transforms continuously between the two states.

A. Two-domain subunit

Figure 2(a) shows the potential describing the states with closed and open domains. When force $f=0$, the closed state "1" is more stable than open state "2," i.e., the height of the barrier ΔE_{12}^0 leading from "1" to "2" is larger than the height of the barrier ΔE_{21}^0 leading from "2" to "1." The force tilts the potential and makes the open state "2" lower in energy than the closed state "1." The solid and dashed lines illustrate these two cases for $f=0$ and $f>f_0=(\Delta E_{12}^0-\Delta E_{21}^0)/2x_d$, where x_d is the barrier width, as explained in detail below. As the force grows from zero to infinity, the potential changes continuously between these two cases. Note that the change in the potential-energy profile for $f\neq 0$ relative to $f=0$ depends on the choice of the origin $x=0$. In Fig. 2(a) the origin coincides with the intersection of the two potential-energy curves.

One should point out that the experimental data obtained for the FimH/mannose system suggests existence of an intermediate state, in addition to the attached and separated states [37]. This intermediate state is short lived, though. Since the rate constants for the transitions from the short-lived state to the other states are significantly larger than the remaining rate constants, the intermediate state can be eliminated from the theoretical analysis without loss of generality.

Let $P_1(t,f)$ denote the probability that the domains are in the attached state "1" at time t and force f. $P_2(t,f)$ denotes the corresponding quantity for the separated state "2." The probabilities evolve in time according to

$$\frac{dP_1(t,f)}{dt} = -k_{12}(f)P_1(t,f) + k_{21}(f)P_2(t,f),$$

$$\frac{dP_2(t,f)}{dt} = -k_{21}(f)P_2(t,f) + k_{12}(f)P_1(t,f), \qquad (1)$$

where $k_{12}(f)$ and $k_{21}(f)$ are the rate constants describing transitions from state "1" to state "2" and back. Following Ref. [11], the force dependence of these rate constants is described by

$$k_{12}(f) = k_{12}^0 \exp\left(\frac{x_d f}{k_B T}\right), \quad k_{21}(f) = k_{21}^0 \exp\left(\frac{-x_d f}{k_B T}\right), \qquad (2)$$

where k_{12}^0 and k_{21}^0 are the rate constants in the absence of force, k_B is the Boltzmann's constant, and T is temperature. The distances from the bound-state minima to the top of the barrier are assumed identical for the forward and reverse processes and equal to x_d. The assumption reflects the fact that the domains displace by the same amount when opening and closing. Since the two-domain system exists either in state "1" or in state "2," the probabilities add up to one,

$$P_1(t,f) + P_2(t,f) = 1. \qquad (3)$$

The solution of Eqs. (1) subject to constraint (3) and condition $f=const$ is

$$P_1(t,f) = a(f) + b(f)\exp\{-t/\tau_d\}, \qquad (4)$$

where

$$\tau_d(f) = \frac{1}{k_{12}(f) + k_{21}(f)} \qquad (5)$$

is the characteristic relaxation time in the two-domain system. The parameters $a(f)$ and $b(f)$ are defined by

$$a(f) = \frac{k_{21}(f)}{k_{12}(f) + k_{21}(f)}, \quad b(f) = a(0) - a(f). \qquad (6)$$

$a(0) \equiv P_1(0,0)$ is the probability to be in state "1" at the initial time and zero force.

B. Receptor/ligand interaction

The probabilities $P_1(t,f)$ and $P_2(t,f)$ for the domains to be attached or separated determine the depth of the potential well describing the receptor/ligand interaction (Fig. 2(b)). The interaction potential contains one minimum and one barrier. The depth of the minimum fluctuates between states "1" and "2," in correspondence with states "1" and "2 of the two-domain subunit. State "2" of the receptor/ligand interaction potential corresponds to the stretched interdomain conformation and is deeper than state "1." Therefore, the rate constant $k_1(f)$ describing the escape of the ligand from minimum "1" is larger than the rate constant $k_2(f)$ for the ligand escape from minimum "2," $k_1(f)>k_2(f)$. This remains true for all force values. The dependence of these rate constants on force is given by the Bell expression [11]

$$k_1(f) = k_1^0 \exp(x_r f/k_B T), \quad k_2(f) = k_2^0 \exp(x_r f/k_B T), \quad (7)$$

and is due to the usual lowering of the barrier by the applied force. Here, k_1^0 and k_2^0 are the rate constants at zero force, and x_r is the distance from the minimum to the maximum. It is chosen to be identical for potentials "1" and "2."

The ligand experiences an average potential, according to the probabilities of the two-domain subunit to exist in the attached or separated states, $P_1(t,f)$ and $P_2(t,f)$, respectively. The average bond-dissociation rate constant is equal to

$$k_r(t,f) = k_1(f)P_1(t,f) + k_2(f)P_2(t,f). \quad (8)$$

Taking into account Eqs. (3) and (4), Eq. (8) can be rewritten in the form

$$k_r(t,f) = \frac{1}{\tau_c(f)} + b(f)[k_1(f) - k_2(f)]\exp(-t/\tau_d), \quad (9)$$

which explicitly demonstrates the time dependence of the rate constant. The time $\tau_c(f)$ introduced in Eq. (9) is defined by

$$\tau_c(f) = \frac{1}{k_2(f) + a(f)[k_1(f) - k_2(f)]}. \quad (10)$$

As will be shown below, this time characterizes the lifetime of the receptor/ligand bond.

The probability $P(t,f)$ that the ligand is bound to the receptor satisfies equation

$$\frac{dP(t,f)}{dt} + k_r(t,f)P(t,f) = 0. \quad (11)$$

The solution of this equation subject to the initial condition $P(0,f)=1$ is given by

$$P(t,f) = C \exp\{-t/\tau_c(f) + b(f)[k_1(f) - k_2(f)]\tau_d(f) \times \exp[-t/\tau_d(f)]\}, \quad (12)$$

where $C=\exp\{-b(f)[k_1(f)-k_2(f)]\tau_d(f)\}$. Thus, the probability for the complex to exist in the bond state at time t and force f, Eq. (12), depends on two characteristic times $\tau_c(f)$ and $\tau_d(f)$, as observed in the FimH/mannose experiments [38]. The probability density of bond rupture $p(t,f)=-\partial P(t,f)/\partial t$ at a given time with fixed force also depends on these characteristic times.

The bond lifetime $\bar{\tau}(f)$ as a function of force is defined in general by

$$\bar{\tau}(f) = \int_0^\infty P(t,f)dt. \quad (13)$$

The integral in Eq. (13) can be computed numerically. An analytic solution can be found by taking into account the experimental fact that the time evolution of the probability $P(t,f)$ exhibits a fast component at early times and a slow component at long times [38]. According to this observation, the characteristic time for the two-domain system $\tau_d(f)$ must be significantly shorter than time $\tau_c(f)$, which determines the overall lifetime of the complex, $\tau_d(f) \ll \tau_c(f)$. This implies that on the time scale given by $\tau_c(f)$ the two-domain system has relaxed, and the probabilities $P_1(t,f)$ and $P_2(t,f)$ have reached their equilibrium values. Neglecting the time-dependent term in Eq. (4) gives the equilibrium solution of Eq. (1) for $dP_1/dt=0$ and $dP_2/dt=0$, namely, $P_1(f)=a(f)$. Under this condition, Eq. (12) for the probability of the receptor/ligand complex to exist in the bound state greatly simplifies,

$$P(t,f) = \exp[-t/\tau_c(f)], \quad (14)$$

and Eq. (13) shows that the bond lifetime is equal to $\tau_c(f)$,

$$\bar{\tau}(f) = \tau_c(f). \quad (15)$$

In order to demonstrate that the current model indeed describes catch-binding, Eq. (10) for $\tau_c(f)$ and, hence, for the bond lifetime, can be rewritten in a more explicit form

$$\frac{1}{\tau_c(f)} = k_1^0\left[\alpha + \frac{1-\alpha}{1+\beta\exp(2x_d f/k_B T)}\right]\exp(x_r f/k_B T). \quad (16)$$

This expression contains the ratio of the bond-dissociation rate constants for states "2" and "1," $\alpha=k_2^0/k_1^0$, and the ratio of the forward and backward rate constants for the conformational change of the two-domain fragment, $\beta=k_{12}^0/k_{21}^0$. Both ratios are evaluated at zero force. The bond lifetime defined by Eq. (16) depends on five parameters, k_1^0, α, β, x_d, and x_r, which can be found by fitting experimental data, as illustrated below with the P-selectin/PSGL-1 and FimH/mannose catch bonds.

C. Further analysis of the catch-bond lifetime

Application of Eq. (16) to experimental data can be simplified by the following observations. Both experiment and simulation indicate that the two-domain subunits, lectin/EGF in P-selectin [23,34,39] and lectin/pilin in FimH [15,22], exist in the attached state in the absence of force with a nearly 100% probability. This implies that minimum "1" in Fig. 2(a) is significantly deeper than minimum "2." Therefore, $\beta \ll 1$ in Eq. (16). Similarly, experiments show that catch-bond lifetimes are significantly shorter at small forces than at moderate forces. The lifetime enhancement ratio by the catch-binding mechanism can be as high as 120 [21]. Therefore, minimum "1" in Fig. 2(b) is much shallower than minimum "2," and $\alpha \ll 1$ in Eq. (16). Further, one can assume that distance x_d characterizing the large-scale rearrangement of the two domains is significantly greater than distance x_r characterizing the receptor/ligand displacement resulting in bond rupture. Therefore, $2x_d \gg x_r$ in the exponents of Eq. (16).

The above considerations lead to the following simple analytic expression for the force maximizing the bond lifetime:

$$f_{\max} \approx \frac{k_B T}{2x_d}\ln\frac{2x_d}{\alpha\beta x_r}. \quad (17)$$

Catch-bond lifetimes grow initially with increasing force. This condition imposes the following relationship on the parameters of Eq. (16):

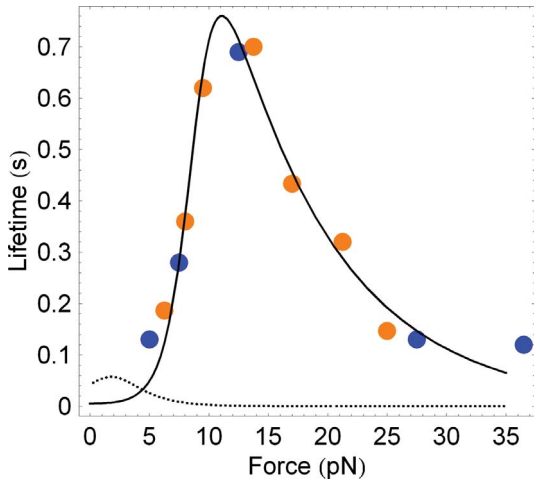

FIG. 3. (Color online) Lifetime of the P-selectin/PSGL-1 complex as a function of applied force. Circles represent the experimental data [12] for monomeric (blue) and dimeric (orange) bonds. The allosteric deformation model predicts that the catch-bond lifetime $\tau_c(f)$ (solid line) is significantly longer than the domain relaxation time $\tau_d(f)$ (dashes).

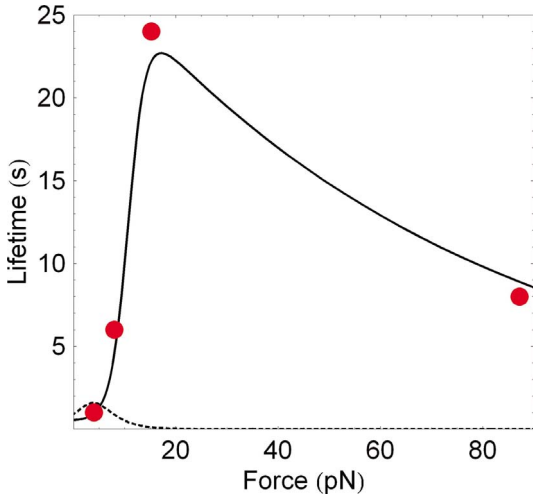

FIG. 4. (Color online) Lifetime of the FimH/mannose complex as a function of applied force. Circles represent the experimental data [22,38]. The bond lifetime (solid line) is much longer than interdomain fragment opening time (dashes), similarly to the P-selectin/PSGL-1 system (Fig. 3).

$$2\beta x_d > x_r, \tag{18}$$

which must be satisfied to create catch-binding.

Finally, in the slip-bond limit of $f \gg f_{\max}$, Eq. (16) has the following asymptotic form:

$$\frac{1}{\tau_c(f \gg f_{\max})} = \alpha k_1^0 \exp\left(\frac{x_r f}{k_B T}\right). \tag{19}$$

In particular, Eq. (19) is useful for analysis and fitting of experimental data.

III. RESULTS

In this section, we apply the allosteric catch-binding model to the experimental data for the P-selectin/PSGL-1 [12] and FimH/mannose [15,22,30,38] complexes and determine the five parameters that define the bond lifetime as a function of applied force, Eq. (16).

A. P-selectin/PSGL-1 bond

Figure 3 shows the lifetimes of the P-selectin/PSGL-1 complex determined experimentally [12] and with the current model as a function of constant force. Ref. [12] considered two types of P-selectin complexes. The binding in the P-selectin/PSGL-1 system was dimeric and involved two identical single bonds. The binding in the P-selectin/sPSGL-1 complex was monomeric. According to the analysis presented in Ref. [21], the dimeric data could be rescaled to correspond to the monomeric case (see Eq. (18) of Ref. [21]). The mean bond lifetimes for the scaled dimeric and original monomeric data of Ref. [12] are depicted in Fig. 3 by the orange and blue circles, respectively. The theoretical analysis of the experimental data was performed using the MATHEMATICA 7.0 software. The solid line in Fig. 3 gives the theoretical lifetime, Eq. (16), for the following parameters $k_1^0=220\ \mathrm{s}^{-1}$, $\alpha=0.0016$, $\beta=0.19$, $x_r=4.4$ Å, and $x_d=18.6$ Å at room temperature $k_BT=40.8$ pN Å. Note that all conditions and assumptions on the parameter values discussed in Sec. II are satisfied. In particular, both α and β are less than one, the distance characterizing the two-domain motion, x_d, is greater than the width of the bond-dissociation barrier, x_r, and the catch-binding condition, Eq. (18), is obeyed. The model gives good agreement between theory and experiment.

The dashed line in Fig. 3 presents the relaxation time for the two-domain fragment, Eq. (5), for the following value of $k_{21}^0=20\ \mathrm{s}^{-1}$. This value is chosen based on the experimental observation that the time evolution of the rupture probability of the P-selectin/PSGL-1 bond follows a single-exponential dependence up to time $0.05\ \mathrm{s}=1/k_{21}^0$ [12]. The domain relaxation time is much shorter than the bond lifetime. The latter, $\bar{\tau}(f) \approx \tau_c(f)$, shows little dependence on the domain relaxation time, $\tau_d(f)$, as established by the above theoretical analysis.

The key characteristics of the receptor/ligand binding potential obtained within the allosteric model for the slip regime directly agree with the corresponding parameters of the two-pathway and deformation models. In particular, the zero-force dissociation rate constants and barrier widths determined for the P-selectin/PSGL-1 bond in the slip limit $f \gg f_{\max}$ are $k_2^0=0.35\ \mathrm{s}^{-1}$ and $x_r=4.4$ Å in the allosteric model, Eq. (16); $0.25\ \mathrm{s}^{-1}$ and 5.1 Å in the two-pathway model [21]; and $0.13\ \mathrm{s}^{-1}$ and 5.7 Å in the deformation model [25]. The parameters describing the catch regime also agree between the three models, even though further steps must be undertaken for the comparison due to the differences in the details of the interpretations of catch-binding (see Sec. IV). The models agree because they all reflect the fundamental physical principle of catch-binding—the depth of the receptor/ligand binding potential grows with increasing force.

B. FimH/mannose bond

Figure 4 presents the experimental data for the FimH/mannose complex obtained by studying FimH mediated adhesion of *Escherichia coli* to mannosylated surfaces [22,38]. The bond lifetimes were obtained by analyzing the duration of bacteria pauses on the model surface at various shear stresses. The drag force f on a stationary sphere touching a wall as a function of shear stress s was determined using the relationship $f=1.7\times 6\pi sr^2$, where the particle radius r was chosen equal to 0.5 μm. The red circles in Fig. 4 show the bond lifetime as a function of constant applied force reported in Ref. [22,38]. The theoretical solid line is derived using Eq. (16) with the following parameters $k_1^0=2$ s^{-1}, $\alpha=0.02$, $\beta=0.1$, $x_r=0.56$ Å, and $x_d=12$ Å. Similarly to the P-selectin/PSGL-1 bond, the assumptions and conditions on the parameter values discussed in Sec. II remain valid. The dashed line gives the relaxation time of the two-domain subunit, Eq. (5), for $k_{21}^0=1$ s^{-1} [38]. The domain relaxation time is much smaller than the bond lifetime and has little effect on the magnitude of the latter.

It is important to note that the allosteric regulation of the receptor/ligand bond via the two-domain fragment is reflected in Eq. (16) by the two parameters β and x_d, which define the term $\beta\exp(2x_df/k_BT)$ in the denominator. These two parameters must satisfy Eq. (18) in order for the bond to exhibit the catch behavior.

IV. RELATIONSHIP OF THE ALLOSTERIC MODEL TO THE GENERAL DEFORMATION MODEL

The allosteric model of the biological catch bond proposed in this work can be regarded as a specific realization of the force-induced bond deformation model developed in Ref. [25]. The allosteric mechanism rationalizes how large-scale changes in the protein structure created by pulling and stretching can propagate to the binding site and affect its properties. The relationship between the two models becomes more apparent by investigating in more detail the effect of the conformational change in the two-domain subunit on the receptor/ligand binding potential. The allosteric force-induced change in the depth of this potential can be expressed within the current model as

$$\Delta E_c(f)=(\Delta E_2-\Delta E_1)[P_2(f)-P_2(0)], \tag{20}$$

where ΔE_1 and ΔE_2 are the depths of the binding potential in states "1" and "2" [see Fig. 2(b)]. Since the force lowers not only the bottom of the well by the allosteric mechanism, but also the top of the barrier according to the Bell mechanism, the overall change in the barrier height as a function of the applied force is

$$\Delta E(f)=\Delta E_0+\Delta E_c(f)-x_rf, \tag{21}$$

where $\Delta E_0=(\Delta E_1+\beta\Delta E_2)/(1+\beta)$ is the barrier height in the absence of the force. Since state "1" is shallower than state "2," Fig. 2(b), $\Delta E_2\gg\Delta E_1$, and Eq. (20) can be expressed as

$$\Delta E_c(f)=\Delta E_2\beta[1-\exp(-2x_df/k_BT)]/[\beta+\exp(-2x_df/k_BT)]. \tag{22}$$

It follows from Eq. (22) that the drop of the bottom of the well by the allosteric mechanism is linear with applied force when the force is small and saturates, reaching the maximum value ΔE_2 at large forces, $f\gg f_0$. These properties of Eq. (22) are entirely analogous to the properties of the bond deformation energy discussed in Ref. [25].

V. DISCUSSION AND CONCLUSIONS

The allosteric model of the biological catch bond proposed in this work emphasizes the central role that the two-domain subunit of the receptor protein plays in determining the receptor/ligand bond lifetime. The model employs only one pathway for bond dissociation, as typically expected with the majority of receptor/ligand systems. The potential experienced by the ligand along this pathway fluctuates, depending on the conformation of the two-domain fragment. In particular, one can expect that the binding site is coupled to a rigid fragment of the receptor protein, such as an α coil or a β sheet, and that force displaces this fragment relative to another rigid structure within the receptor [Fig. 1(a)]. The large-scale conformational rearrangement of the protein propagates onto the binding pocket and changes its shape. As a result, the receptor and ligand better fit each other, and their interaction strengthens.

The allosteric interaction between the two-domain subunit and the binding site acts in both directions. Not only the change in the two-domain conformation affects ligand's binding affinity, but the receptor/ligand bond affects receptor's conformation. In particular, bond dissociation terminates the action of the force, and the two-domain fragment returns to its original closed state. By itself, ligand binding can displace the conformational equilibrium of the receptor protein.

It is essential for catch-binding that the allosteric effect of the two-domain subunit on the binding pocket suppresses the traditional Bell effect within a certain range of applied forces. The bond becomes stronger by the allosteric mechanism, in spite of the lowering of the top of the dissociation barrier by the Bell mechanism. This situation is analogous to the more traditional form of allostery initiated by a control molecule acting as an activator. The opposite situation of the control molecule acting as an inhibitor should have force-induced analogs as well. In this case, the receptor/ligand bond will be weakened by both allosteric and Bell effects. Therefore, such allosteric slip bonds are much harder to detect experimentally than allosteric catch bonds.

It is important to emphasize that a significant fraction of the work performed by the applied force goes to stretch the protein and change its conformation. Only part of the work acts to break the bond. The rest increases the protein energy. At small forces the work performed by the force and, therefore, the total energy of the complex grow as force squared. At the same time, the receptor/ligand interaction energy changes linearly with force, remaining negative, as shown

here and in Ref. [25]. This creates an apparent violation of the energy conservation law. Obviously, it is not true. Reference [25] explains that the negative change in the receptor/ligand interaction energy is offset by a positive change of the protein internal energy, which is stored in the protein deformation. Within the present model, this energy is accumulated primarily in the conformational rearrangement of the two-domain subunit of the receptor.

ACKNOWLEDGMENTS

The authors are grateful to Wendy Thomas for multiple and insightful discussions. Financial support of National Science Foundation under Grant No. CHE-0701517, National Institute of Health under Grant No. NIH R01 AI50940, and Petroleum Research Fund of the American Chemical Society under Grant No. 46772-AC6 is gratefully acknowledged.

[1] J. Monod, J. Wyman, and J. P. Changeux, J. Mol. Biol. **12**, 88 (1965).
[2] D. E. Koshland, G. Nemethy, and D. Filmer, Biochemistry **5**, 365 (1966).
[3] L. T. May *et al.*, Annu. Rev. Pharmacol. Toxicol. **47**, 1 (2007).
[4] A. Cooper and D. T. F. Dryden, Eur. Biophys. J. **11**, 103 (1984).
[5] D. Kern and E. R. P. Zuiderweg, Curr. Opin. Struct. Biol. **13**, 748 (2003).
[6] R. J. Hawkins and T. C. McLeish, Phys. Rev. Lett. **93**, 098104 (2004).
[7] B. Choi *et al.*, Phys. Rev. Lett. **95**, 078102 (2005).
[8] B. Choi and G. Zocchi, J. Am. Chem. Soc. **128**, 8541 (2006).
[9] B. Choi and G. Zocchi, Biophys. J. **92**, 1651 (2007).
[10] S. K. Silverman, Mol. Biosyst. **3**, 24 (2007).
[11] G. I. Bell, Science **200**, 618 (1978).
[12] B. T. Marshall *et al.*, Nature (London) **423**, 190 (2003).
[13] O. Yakovenko *et al.*, J. Biol. Chem. **283**, 11596 (2008).
[14] M. Dembo *et al.* Proc. R. Soc. London, Ser. B **234**, 55 (1988).
[15] W. E. Thomas *et al.*, Cell **109**, 913 (2002).
[16] K. K. Sarangapani *et al.*, J. Biol. Chem. **279**, 2291 (2004).
[17] B. Guo and W. H. Guilford, Proc. Natl. Acad. Sci. U.S.A. **103**, 9844 (2006).
[18] D. Bartolo, I. Derenyi, and A. Ajdari, Phys. Rev. E **65**, 051910 (2002).
[19] E. Evans *et al.*, Proc. Natl. Acad. Sci. U.S.A. **101**, 11281 (2004).
[20] V. Barsegov and D. Thirumalai, Proc. Natl. Acad. Sci. U.S.A. **102**, 1835 (2005).
[21] Y. V. Pereverzev *et al.*, Biophys. J. **89**, 1446 (2005).
[22] W. Thomas *et al.*, Biophys. J. **90**, 753 (2006).
[23] C. Zhu, J. Z. Lou, and R. P. McEver, Biorheology **42**, 443 (2005).
[24] F. Liu, Z. C. Ou-Yang, and M. Iwamoto, Phys. Rev. E **73**, 010901 (2006).
[25] Y. V. Pereverzev and O. V. Prezhdo, Phys. Rev. E **73**, 050902 (2006).
[26] Y. V. Pereverzev *et al.*, Phys. Rev. E **72**, 010903 (2005).
[27] Y. V. Pereverzev and O. V. Prezhdo, Biophys. J. **91**, L19 (2006).
[28] Y. V. Pereverzev and O. V. Prezhdo, Phys. Rev. E **75**, 011905 (2007).
[29] D. E. Koshland, Angew. Chem. Int. Ed. Engl. **33**, 2375 (1994).
[30] W. E. Thomas *et al.*, Mol. Microbiol. **53**, 1545 (2004).
[31] P. Aprikian *et al.*, J. Biol. Chem. **282**, 23437 (2007).
[32] L. M. Nilsson *et al.*, Structure **16**, 1047 (2008).
[33] J. Z. Lou and C. Zhu, Biophys. J. **92**, 1471 (2007).
[34] K. N. Gunnerson, Y. V. Pereverzev, and O. V. Prezhdo, J. Phys. Chem. B **113**, 2090 (2008).
[35] T. T. Waldron and T. A. Springer, Proc. Natl. Acad. Sci. U.S.A. **106**, 85 (2009).
[36] T. A. Springer, Proc. Natl. Acad. Sci. U.S.A. **106**, 91 (2009).
[37] E. V. Sokurenko, V. Vogel, and W. E. Thomas, Cell Host and Microbe **4**, 314 (2008).
[38] W. E. Thomas, V. Vogel, and E. Sokurenko, Annu. Rev. Biophys. **37**, 399 (2008).
[39] J. Z. Lou and C. Zhu, Biophys. J. **92**, 1471 (2007).